CRACK SIZE DEPENDENCE OF THE DUCTILE FRACTURE BEHAVIOUR OF A HIGH STRENGTH STEEL

C. Betegón*, C. Rodríguez† and F.J. Belzunce*

A ductile medium strength steel has been modelled by means of the Gurson's model, and been used to investigate the effect of crack tip constraint in several fracture mechanics specimens. Both numerical and experimental results have been obtained, in the course of the crack extension process, for single edge notch bending specimens with different crack length to width ratios. The geometries with the shorter cracks exhibited higher J values at initiation and steeper J crack growth resistance curves.

INTRODUCTION

Numerous theoretical and experimental studies have demonstrated the inability of single-parameter fracture mechanics to predict structural behaviour in geometries with small cracks. The failure mechanism of ductile tearing is dominated by the nucleation, growth and coalescence of microscopic voids. One of the most commonly used ductile damage models is that of Gurson (1), where the material is regarded as a continuum, damage is described by a single parameter, the void volume fraction or porosity, and the failure process is the result of a local loss of stiffness as the void volume fraction exceeds a certain critical value, f_c, over a certain critical distance, l_c. Both numerical and experimental results will be obtained for single edge notch bending specimens with

*Department of Mechanical Engineering, University of Oviedo
†Instituto Tecnológico de Materiales de Asturias

different crack length to width ratios. The results will be explained in terms of stress and strain fields and damage development.

R-CURVES

Experimentally obtained load-displacement curves were used to calculate the J-integral values. All the load-displacement records were non-linear, and the plasticity at the crack tip was always very extensive. The J integral was determined from the procedure described in the ASTM E813 standard (2) using repeated partial unloadings in order to facilitate the determination of crack growth by the elastic compliance technique. The instantaneous J value was obtained from the splitting of J from its elastic and plastic components. The elastic component was obtained from the stress intensity factor, and the plastic component is given by

$$J_p = \frac{\eta_p U_p}{B(W-a)} \qquad (1)$$

where B and W the thickness, and width specimen, respectivelty and U_p is the plastic component of the area under the load-displacement curve. The η_p parameter for SENB specimens has been obtained by Kirk and Dodds (3) and depends on the crack to width ratio (a/W) and the strain hardening coefficient.

Numerical R curves were calculated for various bend geometries. In order to apply Gurson's model to a particular alloy, a set of material parameters must be determined. One set of parameters describes the elastic-plastic matrix material behaviour, and therefore may be determined from conventional tensile tests after fitting, for example, a Ramberg-Osgood law to the experimental stress-strain curve. However, there is a second set of parameters, related to the nucleation and coalescence processes, that need to be described in order to set up the material evolution model. These were determined both by microscopical examination of the undamaged material,and estimated by numerical fitting of finite element analysis to experimental testing.

Plane strain large deformation finite element calculations were carried out using meshes which modelled the complete SENB specimens. The finite element mesh was identified with the

damage cell size, and failure is considered when the void fraction at a material point reaches a critical value at which no more macroscopic stress can be supported. Numerically obtained load-displacement curves were used to calculated the J-integral values, using the procedure described in the experimental section.

RESULTS AND DISCUSSION

Extensive crack growth was observed in the experimental fracture mechanics tests performed with the SENB specimens at room temperature (upper shelf region). Fig. 1 presents the J crack growth resistance curves (J-Δa) experimentally determined at room temperature with the SENB specimens with different crack to width ratios. The results obtained with the three geometries (a/W= 0.11, 0.2 and 0.5) are clearly different, hence in the frame of this work, the J resistance curve cannot be considered to be an intrinsic material property, but strongly depends on the specimen geometry. Initiation values, defined according to the ASTM standard (2) at a crack growth of 0.2 mm, are about 250 kJ/m^2 for the specimens with the longest crack, a/W=0.5, but a twofold increase was observed in the case of the specimens with crack to width ratios (a/W) of 0.15 and 0.2 (about 500 kJ/m^2). The slope of the curves also depends on the specimen geometry, hence the shorter cracks produce steeper J crack growth resistance curves, and consequently, the differences of the measured J values among the tested geometries increase after a certain crack growth. The same effect of constraint on the slope of the J resistance curves has been observed by different investigators in experiments made with a wide range of cracked geometries on several steels which failed in a ductile manner (4,5).

The longest crack bending geometry only just satisfied the $25J/s_0$ ASTM size criterion for the ligament (W-a), and consequently its R curve has to be considered as a materials property under small scale yielding conditions. Nevertheless, the short cracked bending specimens violated the crack length criterion for single parameter characterisation ($as_0/J<25$) before the first extension of the initial crack and in these cases, J is no longer able to fully characterise the stress field ahead of the crack. It has also been demonstrated that single parameter characterisation of bend specimens is lost when a/W<0.3, where the T stress is negative.

Numerical R-curves, determined from Gurson's model, are presented in Fig. 2 for a/w ratios of 0.05, 0.1,0.2, and 0.5 The crack tip position was taken at the last point where the coalescence void fraction, f_c was attained. The first numerically obtained point represented for each one of the geometries corresponds to the failure of the first integration point in front of the crack tip (Δa=0.05 mm), this point being chosen as the crack growth initiation value. A remarkably good correlation was obtained between the experimental and numerical results for the analysed geometries, as can be seen in Fig. 3 (the continuous curve corresponds to the experimental results), thus the numerical model has demonstrated its ability to accurately predict the crack growth behaviour of SENB specimens with different crack to width ratios. Moreover, differences in the stress and strain fields obtained when applying the model to the three geometries can help us to explain the distinct materials behaviour observed in each case. The opening stresses ahead of the crack tip for the a/w=0.1 geometry have been represented in Fig. 4 as a function of the normalised distance (rs_0/J) for different deformation values, defined by the normalised J (as_0/J), which also corresponds to well defined ductile crack extensions, together with the stress field obtained for the a/W=0.5 geometry, labelled SSY.

CONCLUSIONS

A numerical finite element analysis based on Gurson's model has been employed to explain the ductile crack growth of SENB fracture specimens with different crack to width ratios (a/W = 0.05, 0.1, 0.2 and 0.5). A remarkably good correlation has been obtained between the experimental and numerical results (R-curves) for the analysed geometries, so that the model has demonstrated its ability to accurately predict the crack growth behaviour of these specimens.

The crack growth behaviour of the different geometries were dissimilar, the initiation values and also the slope of the R-curves varied with the specimen geometry, due to differences in crack tip constraint, the shorter cracks having higher J values and steeper J crack growth resistance curves. The opening stresses

and triaxiality which operate in the process zone of the short crack specimens are lower than the small scale yielding results (typical of long cracks under bending), and because of differences in crack tip constraint, the deformation states are also quite divergent, even at the point where the crack initiate its first extension. These changes in the stress and strain fields modify the processes of void nucleation and growth, which take place in front of the crack tip, and justify a greater toughness under bending stresses for the specimens with the shorter cracks.

REFERENCES

(1) Gurson A.L., Continuum theory of ductile rupture by void nucleation and growth. Part I, J. Engng. Mater. Tech., **99**, 2-15 (1977)

(2) ASTM E813 Standard test method for J_{Ic}. A measure of fracture toughness, Annual Book of ASTM Standards, Vol.03.01, Philadelphia ,1989

(3) Kirk M.T. and Dodds R.H. J and CTOD estimation equations for shallow cracks in single notch bend specimens, J. of Test. and Eval., **21**, 4, 228-238, 1993

(4) Hancock J.W., Reuter W.G. and Parks D.M., Constraint and toughness parametrised by T, ASTM Symposiun on Constraint and Fracture, Indianapolis, 1991

(5) Brocks W. and Schmitt W., Constraint Effects in Fracture, ASTM STP 1171, 64-718, 1993

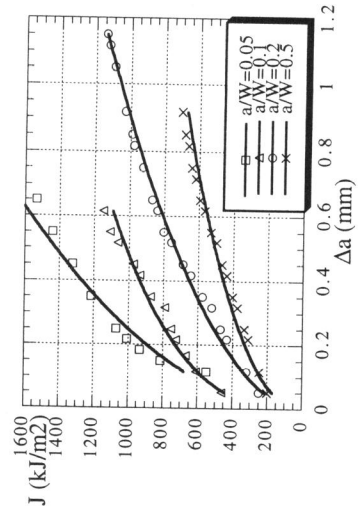

Figure 2. Numerical results

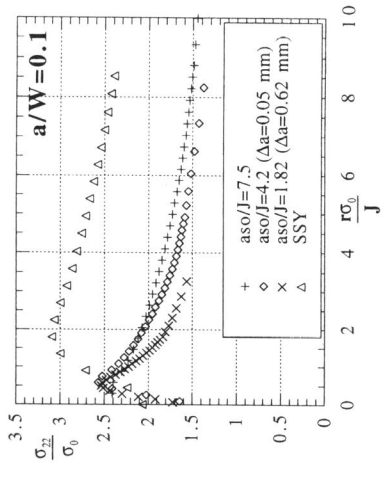

Figure 4. Stresses for the a/W=0.1 specimen

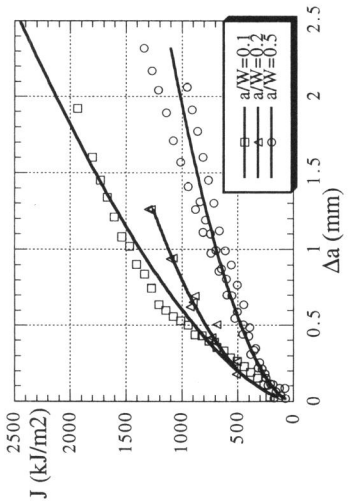

Figure 1. Experimental results

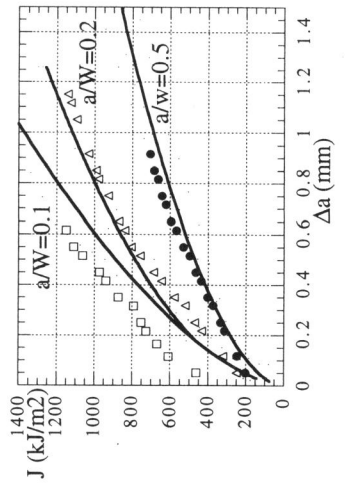

Figure 3. Numerical and experimental results